Automatic Modulation Classification for OFDM Signals based on Deep Learning in Spectrum Sensing

Nahal Maleki
Earth Resource Technologies (ERT)
Greenbelt, MD, USA
nahal.m.tabriz@noaa.gov

Todd Williams
Earth Resource Technologies (ERT)
Greenbelt, MD, USA
todd.williams@noaa.gov

Ulugbek Jainakov
Earth Resource Technologies (ERT)
Greenbelt, MD, USA
ulugbek.jainakov@noaa.gov

Jason Jugar
Earth Resource Technologies (ERT)
Greenbelt, MD, USA
jason..jugar@noaa.gov

Gilberth Caamano
Earth Resource Technologies (ERT)
Greenbelt, MD, USA
gilberth.caamano@noaa.gov

Abstract*—In this study, we focus on classifying the parameters of symbols transmitted over Orthogonal Frequency Division Multiplexing (OFDM) (Cyclic Prefix-OFDM (CP-OFDM) and Discrete Fourier Transform-OFDM (DFT-OFDM)) subcarriers, specifically adhering to 5G uplink specifications. To achieve this, 5G in-phase/quadrature (I/Q) data and measured Signal-to-Noise Ratio (SNR) are input into a convolutional neural network (CNN)-based classifier. Notably, this classifier operates without the need for prior knowledge of protocol-specific information, such as the resource allocation details of 5G physical channels. Our approach has been evaluated using both synthetic and over-the-air datasets. For the over-the-air CP-OFDM I/Q samples, the classifier achieves a minimum accuracy of approximately 0.7 at an SNR of 5 dB, which is higher than the reported state-of-the-art results under similar conditions.

Keywords*—Modulation classification, Spectrum sensing, OFDM, CNN, 5G NR.

I. Introduction

Spectrum sensing is the process of detecting and analyzing signals present in a given frequency band to identify active transmissions and characterize their properties. It plays a key role in applications like cognitive radio, interference management, and spectrum monitoring. One important goal of spectrum sensing is to identify the source of a signal, which involves classifying the signal type (e.g., modulation, protocol) and sometimes estimating parameters such as carrier frequency, bandwidth, and even location. Accurately determining the source helps with efficient spectrum usage, detecting unauthorized transmissions, and ensuring coexistence among wireless systems. Thus, automatic modulation classification (AMC) plays a vital role in spectrum sensing and interference detection. As wireless networks become increasingly complex and heterogeneous, reliable modulation classification is essential for enabling intelligent decision-making at the physical layer.

With the rollout of 5G New Radio (NR) [1], the signal environment has grown more diverse and challenging. 5G employs a flexible numerology, variable subcarrier spacings, diverse bandwidth parts, and multiple physical channels, all of which introduce greater variability in signal characteristics. These complexities make traditional feature-based or likelihood-based AMC approaches less effective, especially under non-ideal channel conditions and real-world impairments.

In recent years, deep learning has emerged as a powerful alternative to conventional signal processing techniques for AMC tasks. By learning directly from raw or minimally processed signal representations, such as I/Q samples or spectrograms, deep neural networks can automatically extract discriminative features and achieve robust performance even in low SNR regimes.

Spectrum sensing presents unique challenges that differ fundamentally from those faced by conventional receivers in wireless networks. While a receiver operates with prior knowledge of the communication protocol and relies on embedded signaling to extract transmission parameters, a spectrum sensor must interpret unknown signals without access to this contextual information.

Modern wireless technologies like 5G rely on OFDM, which introduces a wide range of configurable parameters such as Fast Fourier Transform (FFT) size, cyclic prefix (CP) length, subcarrier spacing (SCS) and OFDM modulation type. These parameters are typically conveyed to the receiver through protocol-specific control messages. However, for spectrum sensing applications, where the goal is to identify signal characteristics passively and without cooperation, some of such protocol-level insights such as SCS, delay and OFDM modulation type are unavailable.

This lack of prior knowledge makes modulation classification particularly difficult. Even when the modulation type is the same, differences in OFDM configurations can alter the signal's time-frequency structure. Therefore, modulation classification in spectrum sensing must be performed directly on the observed data portion of the signal. This constraint motivates the need for learning-based methods capable of generalizing across diverse and unknown signal conditions.

This work explores the use of deep learning for modulation classification of 5G signals. We consider synthetic signals generated via 3rd Generation Partnership Project (3GPP)-compliant test models. The proposed framework is evaluated

across multiple SCS configurations within the frequency range 1 (FR1).

Our results demonstrate that deep learning-based classifiers can effectively generalize across various 5G channel conditions and offer a promising solution for next-generation AMC systems.

There are multiple papers which consider modulation classification using deep learning such as [2]-[8]. All these papers explore various deep learning approaches for modulation classification trying to enhance recognition accuracy with reduced computational complexity which is suitable for cognitive radio.

[9] and [10] investigates the use of deep learning models like Compute library for Deep Neural Networks (CLDNN)s, Long Short-Term Memory (LSTM), and ResNets for modulation classification. It emphasizes techniques to reduce training time, such as Principal Component Analysis and subsampling, while maintaining high classification accuracy.

[11] and [12] propose a Multiple Input Multiple Output (MIMO)-OFDM modulation classification network called 4D2DConvNet for MIMO-OFDM systems. [13] only considers OFDM FFT size estimation and does not consider modulation classification. [14], [17]-[20] only considers 5G downlink signals with lower modulation types not including 256QAM and sometimes not even 64QAM. [15] and [16] assumed that the inputs start from the first sample of the OFDM symbol duration.

[21] provides a survey of deep learning algorithms applied to various OFDM-based systems under different operating conditions. However, to the best of our knowledge, none of the algorithms listed in this paper address 5G uplink or downlink signals, whose frame structures differ significantly from the OFDM formats typically considered in these algorithms and other than that most of the algorithms considered perfect synchronization which is not the case here. Only [22] and [23] include studies on 5G downlink signals. In [23], the focus is limited to classifying CP-OFDM signals with varying symbol lengths, and the modulation scheme is fixed to QPSK, a scenario that differs substantially from our objectives. [22] investigates classification of 5G downlink signals with diverse characteristics. They considered a preprocessing stage to obtain 5G signal feature and these features with the signal are used as the input to a CNN-based classifier. We compare the performance of our proposed method with the results reported

II. System Obectives

OFDM is the core modulation scheme in 5G NR. It splits the available bandwidth into many orthogonal subcarriers, each carrying a low-rate data stream. This approach is highly resistant to frequency-selective fading and makes efficient use of spectrum. CP-OFDM is the baseline waveform in 5G. A short cyclic prefix is added to each OFDM symbol to combat inter-symbol interference caused by multipath propagation. CP-OFDM is used for both downlink and uplink in most cases. DFT-OFDM, also called SC-FDMA, is supported for the uplink in 5G. It adds a DFT precoding step before OFDM modulation, which spreads symbols across subcarriers. This results in a lower peak-to-average power ratio (PAPR), making it more power-efficient for mobile devices.

Fig. 1 illustrates the structure and terminology of the 5G

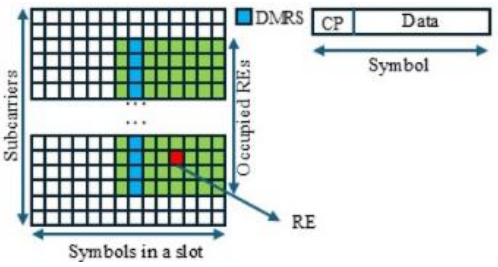

Fig. 1. Resource grid in 5G NR with DMRS and OFDM symbol.

uplink resource grid. A Resource Element (RE) is the most granular unit within this grid defined by the intersection of a single subcarrier in the frequency domain and one OFDM symbol in the time domain. A Physical Resource Block (PRB) comprises 12 consecutive subcarriers in the frequency domain. While the time-domain length of an PRB typically spans one slot, which consists of 14 OFDM symbols.

The number of OFDM symbols per slot, denoted as N, depends on the CP length: the 14 symbols for a normal CP and 12 symbols for an extended CP. But in this paper, we have only considered normal CP thus 14 symbols are in a slot.

In 5G, there are five SCS options, but for Frequency Range 1 (FR1), we consider 15, 30, and 60 kHz.

Each radio frame has a duration of 10 milliseconds and consists of 10 subframes. The blue color in Fig. 1 shows Demodulation Reference Signal (DMRS) which is used for channel estimation. In CP-OFDM signal DMRS always has QPSK modulation but in DFT-OFDM it is Zadoff Chu Sequence.

Our goal is to develop a modulation classifier that utilizes I/Q samples from 5G FR1 uplink signals for spectrum sensing applications. As illustrated in Fig. 2, the system comprises a 5G transmitter (User Equipment (UE) sending signals to a base station. But our receiver antenna continuously monitors the known frequency band, capturing I/Q samples at a sampling rate of f and uses an algorithm and neural network to process the signal. A detection algorithm identifies the OFDM signals and obtains the I/Q samples. We assume accurate detection of 5G signals and every detected OFDM signal applies one modulation scheme for data transmission.

The I/Q samples obtained from the receiver at its original sampling rate, are resampled to a standardized rate that is appropriate for the known channel bandwidth. This resampling aligns with the channel bandwidths of 5G uplink signals, particularly those with Physical Uplink Shared Channel (PUSCH) bandwidths such as 15MHz. By adopting that sampling rate, we ensure that the resampled I/Q sequence fully captures the OFDM signal within our analysis framework. This approach also facilitates straightforward extension to other transmission bandwidths as needed. The resampled I/Q samples, denoted as $y[n]$, serve as inputs to the algorithm detailed in Section C.

A. Data Generation for Training Neural Network

We begin by generating CP and DFT-OFDM I/Q samples using MATLAB's 5G Toolbox. These signal samples include various

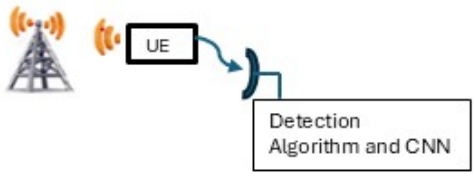

Fig. 2. Modulation classifier system.

modulation schemes commonly used in 5G uplink and downlink transmissions: QPSK, 16QAM, 64QAM, and 256QAM. We excluded π/2-BPSK from our analysis, as it is only used with 5G uplink DFT-OFDM under specific conditions that require a low peak-to-average power ratio.

The generated samples are configured with a fixed number of occupied PRBs and a specific SCS, since they are intended for

training the neural network which will be trained on REs after demodulation of OFDM I/Q data. Given that the operating frequency band is known, the sampling rate is fixed and corresponds to that band. To simulate realistic channel conditions, additive white Gaussian noise (AWGN) is added to the OFDM I/Q samples, with the signal-to-noise ratio (SNR) randomly varied between 0 and 60dB. Then CP-OFDM (and DFT-OFDM) I/Q samples are used as an input to MATLAB's nrOFDMDemodulate function. This command recovers a carrier resource array by demodulating an OFDM modulated waveform, for carrier configuration parameters. The building block for this function can be found [24] and is repeated in Fig. 3. OFDM modulated waveform is a vector of size *T* where *T* is the number of samples in time.

Grid is the output of the function nrOFDMDemodulate and is an array of size *K*-by-*L*. *K* is the number of subcarriers. *L* is the number of OFDM symbols. This function requires prior knowledge of the following parameters:

- NSizeGrid: Number of resource blocks
- SubcarrierSpacing: Subcarrier spacing in kHz
- NSlot: Number of slots in a frame
- CyclicPrefix: Type of cyclic prefix

As channel bandwidth is given in spectrum sensing (In most regions, the channel bandwidth is a predetermined and known value specific to that region) thus NSizeGrid is only dependent on SCS. CyclicPrefix is limited to normal in this paper, and SubcarrierSpacing and occupied REs in the output of the function (grid) are also known in advance only for training purposes. NSlot is also a function of SubcarrierSpacing and thus known in advance. The I/Q samples in each of these REs are considered as demodulated OFDM for CP-OFDM samples. For DFT-OFDM I/Q samples, after this command we should use another IFFT command on occupied REs to obtain demodulated OFDM samples. As mentioned earlier, DMRS in 5G uses QPSK modulation for CP-OFDM and Zadoff-Chu sequences for DFT-OFDM, which can be different from the modulation types used in other REs. However, we cannot simply remove the I/Q samples corresponding to DMRS symbols from the demodulated OFDM data, as the number and location of DMRS symbols in 5G uplink signals can vary

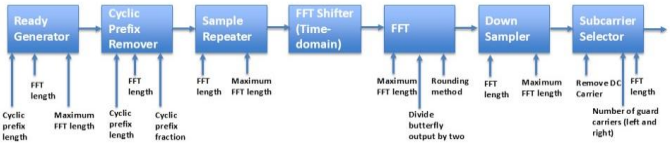

Fig. 3. OFDM demodulator block [24].

significantly. Therefore, we train the network using I/Q samples that include DMRS, even though they may have a different modulation type. Thus, these DMRS symbols with different modulation types can be considered as noise or interference. These demodulated OFDM samples along with the corresponding SNR, serve as input to a CNN. We should note here that we need to generate enough 5G OFDM slots so that after demodulation, there are enough samples to feed into CNN.

Number of occupied REs multiply by number of symbols should be greater than the required number of samples for CNN.

For example, if we need 20,000 samples for training CNN and the number of occupied REs is $50 \times 12 = 600$ (50 is the number of occupied PRBs) then we need at least $\lceil 2000/600 \rceil = 34$ symbols or $\lceil 34/14 \rceil = 3ms$ of data. 80% of the data was allocated for training, and 10% was reserved for validation while the remaining 10% was reserved for testing. The parameters are mentioned in Table I.

B. Neural Network Classifier

These modulated samples along with the corresponding SNR serve as input to CNN. The CNN architecture comprises eight layers, an average pooling layer and a flattening layer at the end, which produces the final output: the predicted modulation type, which is one of the modulation types QPSK, 16QAM, 64QAM and 256QAM and the score related to that modulation type. Solver for training neural network is Stochastic Gradient Descent with Momentum (SGDM) and the number of epochs is set to 14. The learning rate is set to 0.02 at the beginning and the batch size is 256.

The kernel size is 1 × 4, the activation function is Rectified Linear Unit (ReLU) and the layers dimensions versus samples per frame (spf) are mentioned in Table II

C. The Proposed Algorithm

We generate 1000 samples of 5G uplink I/Q data for each modulation scheme, QPSK, 16QAM, 64QAM, and 256QAM, using both CP and DFT-OFDM waveforms. Each set is generated for three SCS values: 15kHz, 30kHz, and 60kHz, using MATLAB's 5G Toolbox. Initially, we assume that both the SCS and the OFDM waveform type are known.

These I/Q samples are passed into MATLAB's nrOFDMDemodulate function, using the given SCS value. The output of this function is a *K*-by-*L* resource grid, where *K* is the number of subcarriers and *L* is the number of symbols. To identify the occupied REs within this grid, the following procedure is used (Alg. 1):

TABLE I. PARAMETERS

Number of I/Q samples generated for each case	1000
Modulation Types	QPSK, 16QAM, 64QAM, 256QAM
SCS (SubcarrierSpacing)	15kHz
Channel Bandwidth	15MHz
Number of PRBs (NSizeGrid)	79
Occupied PRBs	15-64
OFDM Modulation Type	CP-OFDM, DFT-OFDM
Number of slots in a frame (NSlot)	10
Cyclic prefix	Normal
Number of subcarriers (K)	79*12=708
Number of symbols (L)	14*3=42
SNR	Random between 0dB and 60dB
Number of I/Q samples needed for CNN	20000

TABLE II. LAYERS DIMENSIONS AND FILTER SIZES

Operation (BatchNorm, ReLU, MaxPool omitted)	**Output dimension**
Input (IQ imageInputLayer)	[spf × 1 × 2]
Conv2D CNN1 (16 filters)	[spf × 1 × 16]
Conv2D CNN2 (24 filters)	[spf/4 × 1 × 24]
Conv2D CNN3 (32 filters)	[spf/16 × 1 × 32]
Conv2D CNN4 (48 filters)	[spf/64 × 1 × 48]
Conv2D CNN5 (64 filters)	[spf /256× 1 × 64]
Conv2D CNN6 (96 filters)	[spf /1024× 1 × 96]
Conv2D CNN7 (128 filters)	[spf/4096 × 1 × 128]
Conv2D CNN8 (160 filters)	[spf/4^7 × 1 × 160]
AveragePooling2D over time	[1 × 1 × 160]
Flatten	[160]

1. For each symbol *l,* 1,…,L, the power in each of the *k* 1,…,K REs (elements in the resource grid) is calculated and sorted.
2. The difference in power between adjacent REs in the sorted list is computed. Let D_{lk} represent the power difference between RE *k* and its nearest neighbor for symbol *l* when sorted.
3. The root mean square (RMS) of all D_{lk} values is calculated and denoted as D_{rms}.
4. The first RE with a power difference greater than D_{rms} is marked as the start block, and the next one exceeding the threshold is identified as the stop block.
5. This process is repeated across all OFDM symbols.

If the assumed OFDM modulation type is DFT-OFDM, an additional IFFT is applied to the REs located between the identified start and stop blocks in Alg. 1 to recover the time-domain signal.

We should note that this algorithm can also be applied when the occupied PRBs within a symbol are non-contiguous. However, for the sake of simplicity in this paper, we restrict our focus to continuous occupied PRBs.

For each element (RE) in the grid, we calculate its power. If that RE is between the start and stop block, RE is considered part of a signal. If not, the element is considered noise.

We compute the mean power of all elements classified as noise to estimate the noise power and similarly computing the mean power of elements classified as signal to estimate the signal power. The SNR is then calculated as the ratio of signal power to noise power. This SNR value, along with the required demodulated I/Q samples, serves as an input to a neural network designed for further processing or classification tasks.

1) Handling Synchronization Offsets

It's important to note that the I/Q samples received may not be time-synchronized; thus, the first OFDM symbol in a slot does not necessarily align with the start of the time-domain data. To address this, we perform a sliding window analysis over a range of REs. The window should slide one sample each time and in total it should slide by a value equivalent to the duration of one OFDM symbol. This ensures that at least one window position aligns correctly with the start of an OFDM symbol.

For each window position, we repeat the OFDM demodulation and SNR estimation processes described earlier. The resulting data is then passed through the neural network. Among the outputs, we select the modulation type with the smallest constellation size as the final estimated modulation type for the given SCS and OFDM type. The modulation type with the smallest constellation size is chosen as the result. This is because time misalignment can act like noise, making a lower-order modulation appear as a higher-order one with a high score. Therefore, the selection criterion cannot rely on the score. For instance, if the network outputs 256QAM and 16QAM across all window positions, we choose 16QAM as the estimated modulation type. The highest score among all instances of the selected modulation type is taken as the final score, and the corresponding window position (in sample) is used as the estimated delay for that fixed SCS and OFDM types.

2) Handling Unknown SCS and OFDM Types

Since the SCS and OFDM types (CP or DFT-OFDM) are unknown, the entire classification process must be repeated for each possible SCS and OFDM type. The modulation scheme that yields the highest confidence score is selected as the estimated modulation type. Correspondingly, the SCS, OFDM type, and delay values associated with that highest score are taken as the estimated parameters. This approach ensures robust classification, even in the presence of timing misalignments.

Algorithm

Receive I/Q sample and resample to associated sampling rate for that channel bandwidth: $y[n]$
Define *SCS-set*= {15kHz,30kHz,60kHz}
Define *OFDM Mod. Type-set*= {CP, DFT},
for i=1:3 and j=1:2
    SCS= *SCS-set*(i),
    OFDM Mod. type= *OFDM Mod. type-set*(j).
    for each *window position* (*wp*) in a symbol
        Use nrOFDMDemodolate on $\boldsymbol{y}$ covered by that window, $\boldsymbol{y}_{wp}$:
        $\boldsymbol{d}$ = nrOFDMDemodolate ($\boldsymbol{y}_{wp}$).
        Use Alg. 1 to find occupied PRBs:
        $\boldsymbol{s}$ = $\boldsymbol{d}$ (occupied PRB).
        if *OFDM Mod. type-set*(j) = DFT
            Use IFFT on data: $\boldsymbol{s}$ = IFFT($\boldsymbol{s}$).
        end
        Use Alg. 2 to find SNR_s =SNR of $\boldsymbol{s}$
        $\mathbf{s}$ and SNR_s: input to CNN.
        mod(*wp*)= chosen modulation type by CNN.
        score(*wp*)=score of chosen modulation type.
        cons(*wp*)=constellation size of *mod*(*wp*).

end
$mDelay(i,j) = \arg min_{wp}\,(cons)$.
mMod(i,j)=*mod*(*mDelay*)
mScore(i,j)=*score*(*mDelay*).
end
$(fSCS, fofdmMod) = \arg max_{i,j}\,(score)$.
$fMod = mMod(fSCS, fofdmMod)$.
$fDelay = mDelay(fSCS, fofdmMod)$.
$fSCS$, $fofdmMod$, $fMod$ and $fDelay$ are the final estimated SCS, OFDM modulation type, modulation type and delay.

III. Simulation Results

The proposed classifier is evaluated using synthetic and over-the-air data. Synthetic data is generated using MATLAB R2023a with the 5G Toolboxes over an AWGN channel. All three SCS 15kHz, 30kHz and 60kHz are considered. Also, both OFDM modulation types of CP and DFT-OFDM and all modulation types are considered. 1000 samples for each case are generated. For synthetics data SNR is changing from 5dB to 30dB in step of 5dB. As channel bandwidth and thus occupied PRBs in that channel are given, channel bandwidth is set to 15MHz and occupied PRBs are from PRB 15 to PRB 64 without loss of generality. These signals are considered as input OFDM I/Q samples to the proposed algorithm in Section II.C.

A. Evaluation Results

The results shown in Fig. 4-6 are based on synthetic data generated under an AWGN channel. In this section, we report the accuracy of the algorithm in estimating OFDM modulation type, SCS, modulation type and delay respectively. Our results demonstrate near-perfect accuracy in estimating OFDM modulation type (CP or DFT-OFDM) across various SCS and SNR values. Even at low SNR levels, the system maintains high classification accuracy for both modulation types. This outcome is expected, as CP and DFT-OFDM are fundamentally different, making it relatively easy for the neural network to distinguish between them, even under challenging noise conditions.

The simulation results in Table III shows accuracy for different modulation types in estimation SCS when OFDM modulation type is set to CP and DFT-OFDM. From this Table it is also clear that even at low SNR classification accuracy is very high.

Fig. 4 shows the modulation classification accuracy (accuracy in estimating modulation type) for CP-OFDM (and DFT-OFDM) I/Q samples across different modulation types and SNR levels. From this Figure we can conclude that 256QAM has the worst accuracy and also accuracy increases by SNR as expected for all modulation types. Modulation accuracy for CP and DFT-OFDM I/Q samples for the same value of SNR is very similar.

TABLE III. SCS ACCURACY VERSUS SNR FOR CP AND DFT-OFDM

	SNR=5dB	**SNR=10dB**	**SNR=15dB**
15kHz, CP	0.97	1	1
30kHz, CP	0.96	1	1
60kHz, CP	0.98	1	1
15kHz, DFT	0.95	1	1
30kHz, DFT	0.94	1	1
60kHz, DFT	0.97	1	1

Fig. 5 summarizes the overall accuracy for both CP and DFT-OFDM across varying SNR values. From this Figure it is clear that accuracy of DFT-OFDM samples is slightly higher than the one for CP-OFDM samples. When comparing our total accuracy results for CP-OFDM samples to those in Fig. 11 from [21], we observe higher accuracy at lower SNRs. Additionally, [21] includes 1024QAM, a modulation type not considered in our study because we consider 5G uplink signal, but our method still achieves a higher overall accuracy even if we assume zero accuracy for 1024QAM to match conditions in [21].

For brevity, we report modulation classification performance only for the 15 kHz SCS case. Additional experiments conducted with other SCS values (e.g., 30 kHz, and 60 kHz) demonstrated nearly identical qualitative and quantitative trends; therefore, these results are omitted due to space constraints.

Among all these parameters, correctly identifying the modulation type presents the greatest challenge, along with accurately estimating the delay. Fig. 6 shows an average estimated delay versus SNR for both CP-OFDM and DFT-OFDM signals. This Figure illustrates that the delay estimation accuracy for CP-OFDM signals is significantly higher than that for DFT-OFDM. This difference arises because DFT-OFDM is inherently less sensitive to timing delays, multiple delay values can still yield correct modulation classification. This is due to the double transformation process in DFT-OFDM, where an FFT is applied in nrOFDMDemodulate function before the IFFT, making the time delay largely independent of frequency shifts, unlike in CP-OFDM (demodulation process for CP-OFDM samples does not include IFFT thus delays are transformed to frequency shifts). However, this implies that estimating the delay becomes more difficult for DFT-OFDM, as a wide range of delay values may appear equally valid.

Over-the-air datasets are obtained from real-world 5G and 4G Long Term Evolution (LTE) datasets received by Radio Frequency Interference Monitoring System (RFIMS) antenna (44 antenna columns) at Table Mountain Test Range in Boulder CO. 100 samples are collected for each modulation type for CP and DFT-OFDM. We should note here that all LTE signals have DFT-OFDM modulation type, but 5G signals can have both CP and DFT modulation type.

5G signals are collected from 1695-1710MHz band but 4G LTE signals are collected from 1710-1720MHz frequency band.

Fig. 7 shows the spectrogram of a 16ms capture of an LTE signal that has DFT-OFDM and 16QAM modulation. Only 2ms of this capture is used for modulation classification. The output of the algorithm is 16QAM modulation which is a true positive.

Fig. 8 shows overall accuracy versus SNR for over-the-air datasets. From this Figure it is clear that the result of the over-the-air testing is very similar to synthetic data testing.

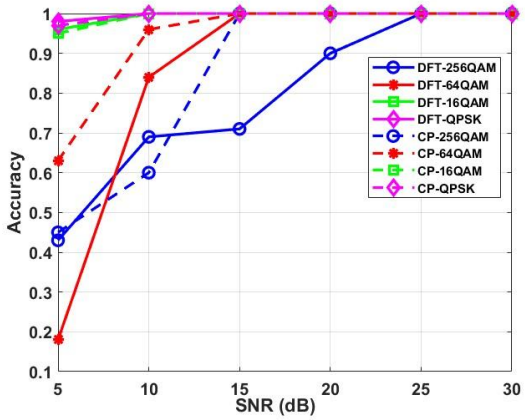

Fig. 4. Modulation type accuracy versus SNR for CP-OFDM and DFT-OFDM I/Q samples for different modulation types.

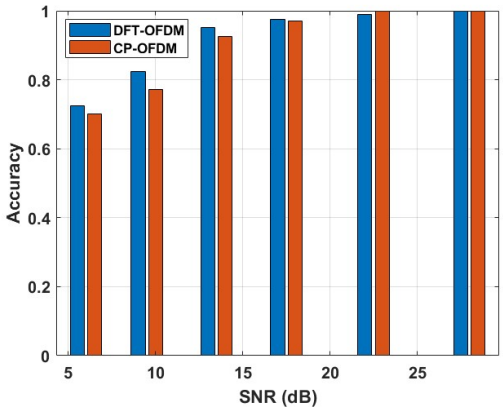

Fig. 5. Total modulation type accuracy versus SNR for CP-OFDM and DFT-OFDM I/Q samples.

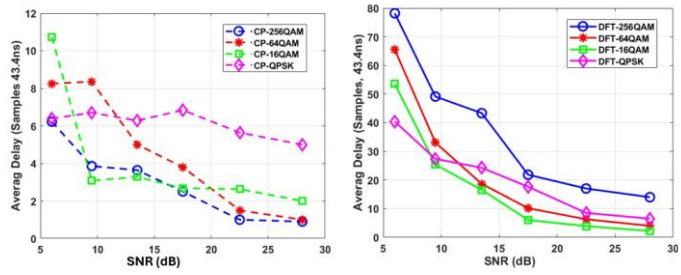

Fig. 6. Estimated delay versus SNR (a) CP-OFDM (b) DFT-OFDM

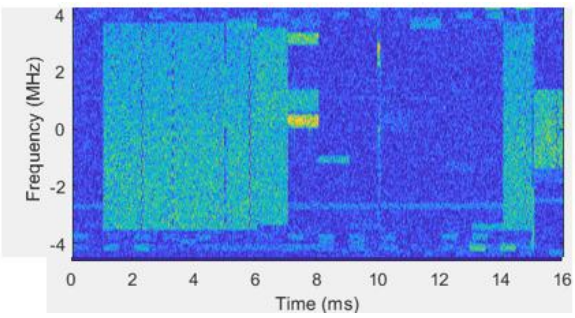

Fig. 7. Spectrogram of an LTE signal in 1710-1720MHz band.

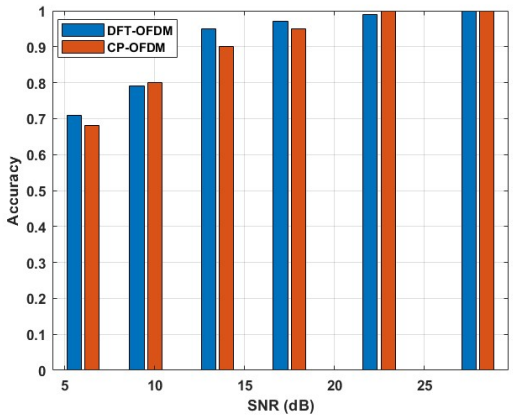

Fig. 8. Total modulation type accuracy versus SNR for CP-OFDM and DFT-OFDM I/Q samples for over-the-air dataset.

IV. Conclusion

In this paper, we evaluated the performance of a neural network for classifying modulation types, SCS, and OFDM waveform formats (CP-OFDM and DFT-s-OFDM) in 5G signals. We also demonstrated that the same network architecture can be extended to estimate time delays in the received samples. Our results show that the proposed model consistently outperforms prior methods, particularly at low SNR levels, an important advantage for spectrum-sensing applications where received signal power is highly unpredictable due to unknown transmitter–receiver separation and varying transmit power.

Beyond MATLAB-generated waveforms and simulated channels, we further validated our approach using over-the-air transmissions that include realistic channel impairments. The performance remained strong under these conditions and exceeded the results reported in existing studies that considered only 5G downlink signals.

Although our primary experiments focus on 4G/5G uplink waveforms, especially PUSCH, the proposed framework can be adapted to downlink channels and other physical-layer signals with minor modifications. The only exception is 1024-QAM, which is outside the scope of this work.

References

[1] 3GPP TR 38.331, “NR; Radio Resource Control (RRC); Protocol specification,” Mar. 2023, ver 17.4.0.

[2] Peng, S., Sun, S. and Yao, Y.D. ”A survey of modulation classification using deep learning: Signal representation and data preprocessing,” IEEE Transactions on Neural Networks and Learning Systems, vol. 33(12), pp.7020-7038, 2021.

[3] M. Ma, Z. Li, Y. Lin, L. Chen, and S. Wang, "Modulation classification method based on deep learning under non-Gaussian noise." In 2020 IEEE 91st Vehicular Technology Conference (VTC2020-Spring), pp. 1-5, 2020.

[4] B. Singh, and C. Prakash, "Deep Learning Enabled Algorithm for Automatic Modulation Classification." In 2024 IEEE Space, Aerospace and Defence Conference (SPACE), pp. 916-921, 2024

[5] G. Jajoo, and P. Singh, "Modulation classification for overlapped signals using deep learning." IEEE Open Journal of the Communications Society, 2024.

[6] S. Kim, J. Kim, V. Doan, and D. Kim, "Lightweight deep learning model for automatic modulation classification in cognitive radio networks." IEEE Access, vol. 8, pp. 197532-197541, 2020.

[7] C. Harper, A., Mitchell A. Thornton, and Eric C. Larson, "Automatic modulation classification with deep neural networks." Electronics, vol. 12, no. 18, pp. 3962, 2023.

[8] V. Doan, T. Huynh-The, C. Hua, Q. Pham, and D. Kim, "Learning constellation map with deep CNN for accurate modulation recognition." In GLOBECOM 2020-2020 IEEE Global Communications Conference, pp. 1-6, 2020.

[9] X. Liu, D. Yang, and A. El Gamal, "Deep neural network architectures for modulation classification." In 2017 51st Asilomar Conference on Signals, Systems, and Computers, pp. 915-919, 2017.

[10] S. Ramjee, S. Ju, D. Yang, X. Liu, A. El Gamal, and Y. C. Eldar, "Fast deep learning for automatic modulation classification." arXiv preprint arXiv:1901.05850 (2019).

[11] B. Ren, K. Chan Teh, H. An, and E. Gunawan, "MIMO-OFDM Modulation Classification Using 4D2DConvNet for 5G Communications." IEEE Wireless Communications Letters, 2024.

[12] T. Huynh-The, T. Nguyen, Q. Pham, D. Benevides da Costa, and D. Kim, "MIMO-OFDM modulation classification using three-dimensional convolutional network." IEEE Transactions on Vehicular Technology, vol. 71, no. 6, pp. 6738-6743, 2022.

[13] M. Park, and D. Han, "Deep learning-based automatic modulation classification with blind OFDM parameter estimation." IEEE Access, vol. 9, pp. 108305-108317, 2021.

[14] A. Kumar, K. Kumar Srinivas, and S. Majhi, "Automatic modulation classification for adaptive OFDM systems using convolutional neural networks with residual learning." IEEE Access, vol. 11, pp. 61013-61024, 2023.

[15] R. Gupta, S. Kumar, and S. Majhi, "Blind modulation classification for asynchronous OFDM systems over unknown signal parameters and channel statistics." IEEE Transactions on Vehicular Technology, vol. 69, no. 5, pp. 5281-5292, 2020.

[16] S. Hong, Y. Zhang, Y. Wang, H. Gu, G. Gui, and H. Sari, "Deep learning-based signal modulation identification in OFDM systems." IEEE Access, vol. 7, pp. 114631-114638, 2019.

[17] T. Huynh-The, T. Nguyen, Q. Pham, D. Benevides da Costa, G. Kwon, and D. Kim, "Efficient convolutional networks for robust automatic modulation classification in OFDM-based wireless systems." IEEE Systems Journal, vol. 17, no. 1 pp. 964-975, 2020.

[18] L. Zhang, C. Lin, W. Yan, Q. Ling, and Y. Wang, "Real-time OFDM signal modulation classification based on deep learning and software-defined radio." IEEE Communications Letters, vol. 25, no. 9, pp. 2988-2992, 2021.

[19] R. Shah, A. Parmar, A. Chouhan, and K. Captain, "OFDM Signal Modulation Classification using Dilated CNN Model." In 2025 17th International Conference on COMmunication Systems and NETworks (COMSNETS), pp. 857-861, 2025.

[20] T. Huynh-The, Q. Pham, T. Nguyen, X. Pham, and D. Kim, "Deep learning-based automatic modulation classification for wireless ofdm communications." In 2021 International Conference on Information and Communication Technology Convergence (ICTC*)*, pp. 47-49, 2021.

[21] A. Kumar, S. Majhi, G. Gui, H.C. Wu, and C. Yuen, "A survey of blind modulation classification techniques for OFDM signals, Sensors, pp.1020, 2022.

[22] B. Kim, C. Mecklenbräuker, and P. Gerstoft, "Deep Learning-based Modulation Classification of Practical OFDM Signals for Spectrum Sensing." In IEEE INFOCOM 2024-IEEE Conference on Computer Communications, pp. 1611-1620, 2024.

[23] J. Combo, A. Tato, J. Joaquín Escudero-Garzás, L. Pérez Roca, and P. González, "Deep Learning based CP-OFDM Signal Classification with Data Augmentation." In 2022 IEEE International Black Sea Conference on Communications and Networking (BlackSeaCom), pp. 352-357, 2022.

[24] https://www.mathworks.com/help/wireless-hdl/ref/ofdmdemodulation